

Doping dependence of the specific heat of single-crystal $\text{BaFe}_2(\text{As}_{1-x}\text{P}_x)_2$

C. Chaparro,¹ L. Fang,¹ H. Claus,¹ A. Rydh,² G. W. Crabtree,^{1,3} V. Stanev,¹ W. K. Kwok,¹ and U. Welp¹

¹Materials Science Division, Argonne National Laboratory, Argonne, Illinois 60439, USA

²Department of Physics, Stockholm University, SE-10691 Stockholm, Sweden

³Department of Physics, University of Illinois at Chicago, Chicago, Illinois 60607, USA

(Received 11 October 2011; published 22 May 2012)

We present specific heat measurements on a series of $\text{BaFe}_2(\text{As}_{1-x}\text{P}_x)_2$ single crystals with phosphorous doping ranging from $x = 0.3$ to $x = 0.55$. Our results reveal that $\text{BaFe}_2(\text{As}_{1-x}\text{P}_x)_2$ follows the scaling $\Delta C/T_c \approx T_c^2$ remarkably well. The clean-limit nature of this material imposes additional restraints on theories aimed at explaining the scaling. Furthermore, we find that the Ginzburg-Landau parameter decreases significantly with doping whereas the superconducting anisotropy is $\Gamma \approx 2.6$, independent of doping.

DOI: [10.1103/PhysRevB.85.184525](https://doi.org/10.1103/PhysRevB.85.184525)

PACS number(s): 74.25.Bt, 74.25.Dw

Empirical relations expressing universal trends in the behavior of classes of materials have proven important in clarifying underlying physical mechanisms. Examples include, among others, the Kadowaki-Woods relation¹ linking the electron effective mass enhancement to the temperature dependence of the resistivity in Fermi liquid systems, and the Uemura plot² and Homes scaling³ establishing relations between the superfluid density and the value of T_c in superconductors. Recently, Bud'ko *et al.*⁴ observed that the specific heat anomaly at the superconducting transition of a series of $\text{Ba}(\text{Fe}_{1-x}\text{Co}_x)_2\text{As}_2$ and $\text{Ba}(\text{Fe}_{1-x}\text{Ni}_x)_2\text{As}_2$ crystals displayed an unexpected scaling of the form $\Delta C/T_c \approx T_c^2$ (BNC scaling). Since then, this scaling has been found to apply in a wide variety of Fe-pnictide and Fe-chalcogenide superconductors; see compilations in Refs. 5 and 6 and also Fig. 5 below. However, a completely satisfying theoretical explanation is still lacking.

Here, we present specific heat measurements on a series of $\text{BaFe}_2(\text{As}_{1-x}\text{P}_x)_2$ single crystals with phosphorus content ranging from near-optimum doped $x = 0.3$ to strongly overdoped $x = 0.55$. In contrast to most other members of the Fe-pnictide and Fe-chalcogenide superconductors, $\text{BaFe}_2(\text{As}_{1-x}\text{P}_x)_2$ can be grown with very high purity as evidenced by the observation of de Haas van Alphen measurements giving detailed knowledge on the electronic structure,^{7,8} and by the low values of critical current density and residual resistivity.⁹ Furthermore, thermal conductivity,¹⁰ NMR,¹¹ penetration depth,¹² and ARPES¹³ measurements indicate the presence of line nodes in the superconducting gap although the detailed gap structure is still controversial. Our specific heat results reveal that $\text{BaFe}_2(\text{As}_{1-x}\text{P}_x)_2$ follows the BNC scaling remarkably well. The high purity of this material imposes additional restraints on theories aimed at explaining the scaling since models based on specific electron scattering mechanisms appear to be inconsistent with our results. We find that the Ginzburg-Landau (GL) parameter κ_c decreases significantly with doping, whereas the superconducting anisotropy is $\Gamma \approx 2.6$, independent of doping, indicative of the dominating role of the electron Fermi surface sheets in forming the superconducting state.

High-purity $\text{BaFe}_2(\text{As}_{1-x}\text{P}_x)_2$ single crystals were grown using a self-flux method. Thoroughly mixed high-purity Ba flakes (99.99%, Aldrich) and FeAs and FeP (homemade from Fe, As, and P, 99.99%, Aldrich) powders were placed in Al_2O_3

crucibles. The crucible was sealed in an evacuated quartz tube under vacuum and heated up to 1180 °C and cooled down to 900 °C at a rate 2 °C/min. This procedure yielded hundreds of crystals with platelet shapes. The largest size is ~ 1 mm, with most crystals ranging in size between 300 and 600 μm . The concentration of phosphorus was determined using x-ray energy dispersive spectra (EDS). Low-field magnetization measurements in a field of 1 G were performed in a custom-built superconducting quantum interference device (SQUID) magnetometer.¹⁴ The measurements were performed on warming after initially cooling in zero field. We performed the caloric measurements using a membrane-based steady-state ac microcalorimeter.¹⁵ It utilizes a thermocouple thermometer composed of Au-1.7% Co and Cu films deposited onto a 150-nm-thick Si_3N_4 membrane. We use zero-field and in-field measurements on Au samples, which have heat capacity that is comparable to that of our samples in order to obtain an accurate calibration of our calorimeter. The current calorimeter works for temperatures above ~ 6 K. The crystals were mounted onto the thermocouple with minute amounts of Apiezon N grease. An ac heater current at a frequency of typically 47 Hz is adjusted such as to induce 50–200 mK oscillations of the sample temperature.

The lower inset of Fig. 1 shows the temperature dependence of the magnetization of the $\text{BaFe}_2(\text{As}_{1-x}\text{P}_x)_2$ single crystals used in this study. The magnetic transition widths are generally less than 1 K, with the sharpest transition being only 200 mK wide, underlining the high quality of the crystals. The top inset of Fig. 1 shows a picture of a cleaved single crystal displaying a flat and shiny surface. The main panel shows the heat capacity of the $x = 0.3$ crystal. A sharp transition is clearly seen in C/T near 29 K. For further analysis of the superconducting specific heat we extrapolate the normal state background as indicated by the dashed line. Although this procedure is not suitable for determining the electronic specific heat at temperatures far below T_c , in the temperature range near T_c the shape of the specific heat anomaly and its field dependence can be extracted reliably. For the heavily overdoped samples ($x = 0.45, 0.50$, and 0.55) a field of 7.9 T $\parallel c$ suppressed superconductivity sufficiently so that these in-field data served as the normal state background.

Figure 2 shows the evolution of the transition in the electronic specific heat of the $x = 0.3$ and $x = 0.5$ crystal in various fields applied parallel to the c axis and parallel

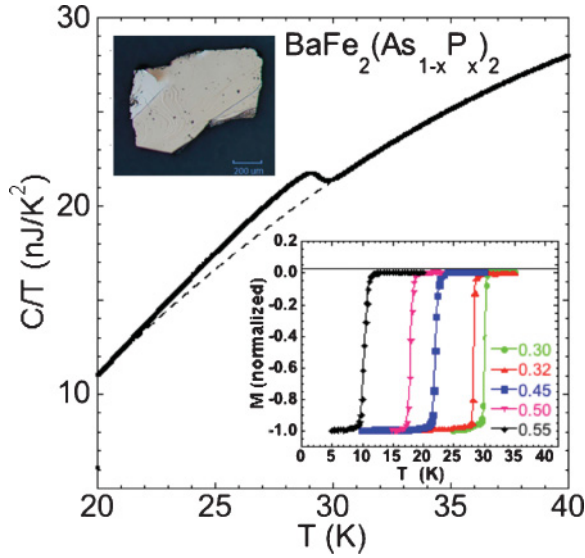


FIG. 1. (Color online) Temperature dependence of the specific heat of $\text{BaFe}_2(\text{As}_{1-x}\text{P}_x)_2$, $x = 0.3$. The dashed line indicates the extrapolation of the normal state background. Lower inset: Temperature dependence of the magnetization of the crystals measured in 1 G $\parallel c$ after cooling in zero field. Top inset: Picture of a cleaved single crystal displaying a shiny and flat surface.

to the ab planes, respectively. In zero field the specific heat anomaly displays a sharp superconducting transition with a width of ~ 1 K which in increasing fields systematically shifts to lower temperatures and broadens weakly. The small broadening in applied fields is consistent with weak superconducting fluctuation effects as quantified by the low value of the Ginzburg number $G_i = (k_B \mu_0 \Gamma T_c / 4\pi \xi_{ab}^3 B_c^2)^2 / 2 = 323.6 (\Gamma \kappa \lambda_{ab} T_c)^2 \approx 5 \times 10^{-5}$ (T in Kelvin, penetration depth λ_{ab} in meters). The in-field behavior of the specific heat anomaly of $\text{BaFe}_2(\text{As}_{1-x}\text{P}_x)_2$ is analogous to that of optimally

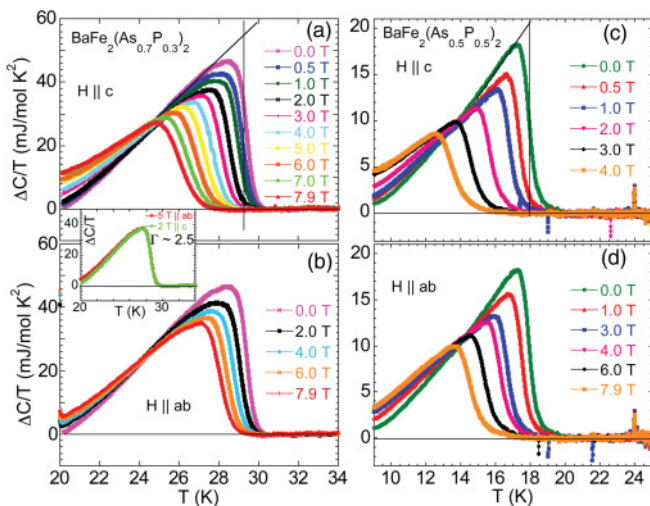


FIG. 2. (Color online) Temperature dependence of the electronic specific heat of $\text{BaFe}_2(\text{As}_{0.7}\text{P}_{0.3})_2$ (a), (b) and $\text{BaFe}_2(\text{As}_{0.5}\text{P}_{0.5})_2$ (c), (d) near the superconducting transition in various fields applied parallel to the c axis and parallel to the ab plane. The solid lines in (a) illustrate the entropy conserving construction used to determine the transition temperature.

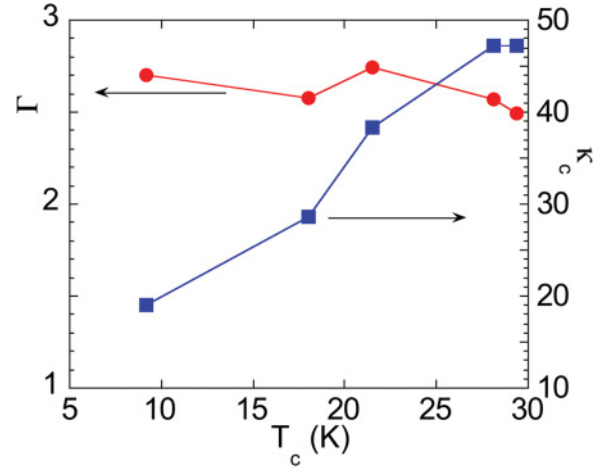


FIG. 3. (Color online) Dependence of the superconducting anisotropy parameter Γ and the c -axis Ginzburg-Landau parameter κ_c on T_c .

doped $\text{Ba}_{1-x}\text{K}_x\text{Fe}_2\text{As}_2$ for which $G_i \approx 10^{-3}$ (Ref. 16) has been estimated, but is in contrast to the pronounced broadening and suppression of the transitions seen in the more anisotropic $\text{SmFeAsO}_{0.85}\text{F}_{0.15}$ and $\text{NdFeAsO}_{0.82}\text{F}_{0.18}$ compounds with $G_i \approx 10^{-2}$.^{17,18}

A comparison of the $H \parallel c$ and $H \parallel ab$ data reveals a superconducting anisotropy of $\Gamma \sim 2.6$, as directly inferred by superimposing the 2 T $\parallel ab$ and 5 T $\parallel c$ data [inset in Figs. 2(a), 2(b)]. We use an entropy conserving construction as indicated by the solid lines in Figs. 2(a) and 2(c) for determining the transition temperature $T_{c2}(H)$ and the height of the specific heat anomaly $\Delta C/T_c$. For the near-optimally doped crystal ($x = 0.30$) we find $\Delta C/T_c = 54$ mJ/mol K^2 whereas for a crystal with $T_c \approx 28$ K, $\Delta C/T_c = 45$ mJ/mol K^2 , which is in good agreement with a value of 38.5 mJ/mol K^2 obtained on an assembly of crystals with similar T_c .⁶ With increasing phosphorus doping T_c/T_c drops significantly to 20 mJ/mol K^2 for the $x = 0.5$ crystal (see below) [Fig. 2(c)]. In the temperature and field range covered here the upper critical field lines, $H_{c2}(T)$, are linear. With the help of the thermodynamic and Ginzburg-Landau relations $\mu_0 \Delta C/T_c = (\mu_0 dH_{c2}/dT)_{T_c}^2 = (\mu_0 dH_{c2}/dT)_{T_c}^2 / \beta_A (2\kappa^2 - 1)$, $\kappa = \lambda_{ab}/\xi_{ab}$, and $\mu_0 H_{c2} = \phi_0 / 2\pi \xi^2$ we evaluate the doping dependence of materials parameters such as κ , coherence length ξ_{ab} , and Ginzburg-Landau penetration depth λ_{GL}^{ab} as listed in Table I.

Figure 3 shows the dependence of the anisotropy parameter Γ and of κ_c upon T_c . Within the experimental uncertainty the anisotropy is independent of T_c , i.e., doping level, at a value of ~ 2.6 . This independence is unexpected since band structure calculations¹⁹ as well as de Haas-van Alphen (dHvA) measurements^{7,8,20} indicate that the c axis dispersion of the outer hole band increases, implying a reduced anisotropy upon doping with P. Our result can be explained if the electron and inner hole bands—which do not change appreciably upon doping—dominate in forming the superconducting state. ARPES experiments on $\text{BaFe}_2(\text{As}_{0.7}\text{P}_{0.3})_2$ (Ref. 13) revealed almost isotropic superconducting gaps of 6–8 meV in the center plane of the Brillouin zone on all five Fermi surface sheets and strong k_z dispersion of the gap on the α -hole

TABLE I. Compilation of the superconducting parameters of samples with various T_c . The values for $\xi_{ab}(0)$ and $\lambda_{GL}^{ab}(0)$ are obtained from the measured upper critical field slopes using a linear extrapolation to zero temperature according to $1/\xi_{ab}^2(0) = (-2\pi T_{c2}/\phi_0)(dH_{c2}/dT)$ and $1/[\lambda_{GL}^{ab}(0)]^2 = 1/[\kappa^2 \xi_{ab}^2(0)]$.

T_c (K)	x	$-\mu_0 dH_{c2}^c/dT$ (T/K)	$-\mu_0 dH_{c2}^{ab}/dT$ (T/K)	Γ	$\Delta C/T_c$ (mJ/mol K ²)	$\mu_0 H_{c2}^c$ (T)	κ	ξ_{ab} (nm)	λ_{GL}^{ab} (nm)
29.2	0.30	-2.44	-6.08	2.49	54.0	71.7	47.3	2.14	101
28.1	0.33	-2.23	-5.73	2.57	45.0	62.7	47.3	2.29	108
21.5	0.45	-1.28	-3.51	2.74	22.0	27.5	38.4	3.46	132
18.0	0.50	-0.90	-2.33	2.58	20.0	16.4	28.6	4.50	129
9.2	0.55	-0.38	-1.00	2.70	8.0	3.5	19.0	9.71	184

Fermi surface suggesting a circular node near the top of the Brillouin zone. Such gap structure may account for the observed doping independence of the anisotropy parameter, even though the detailed gap structure of $\text{BaFe}_2(\text{As}_{1-x}\text{P}_x)_2$ is still controversial.^{10,13} In contrast to Γ , the c -axis GL parameter decreases significantly upon doping; though the material remains clearly type II for all P concentrations (see discussion below).

Figure 4 shows the doping dependence of $\Delta C/T_c$ and $-\mu_0 dH_{c2}^c/dT$. Both quantities are found to be approximately proportional to T_c^2 as indicated by the dotted lines. In a simple analysis, $-\mu_0 dH_{c2}^c/dT|_{T_c} \approx \phi_0/2\pi \xi^2(0)T_c$, which yields for the dirty limit $-\mu_0 dH_{c2}^c/dT|_{T_c} \approx \phi_0/2\pi v_F l$ and $-\mu_0 dH_{c2}^c/dT|_{T_c} \approx \phi_0 T_c/2\pi v_F^2$ in the clean limit. The observation of dHvA oscillations indicates that at least the overdoped samples are close to the clean limit. Neither of these relations agrees with the observed T_c^2 variation; however, in addition to the explicit T_c dependence there may arise unknown implicit T_c dependences due to the doping dependence of Fermi velocity v_F and mean free path l . In the limit of strong pair-breaking scattering and gapless superconductivity, $-\mu_0 dH_{c2}^c/dT \approx T_c$ has been predicted.²¹

The jump height of the specific heat follows a T_c^2 relation reasonably well. In fact, the absolute size of $\Delta C/T_c$ agrees well with the trend observed for a large variety of Fe-pnictide/chalcogenide superconductors as shown in Fig. 5. Even though there may be appreciable deviations in this log-log plot, particularly at low values of T_c and $\Delta C/T_c$,

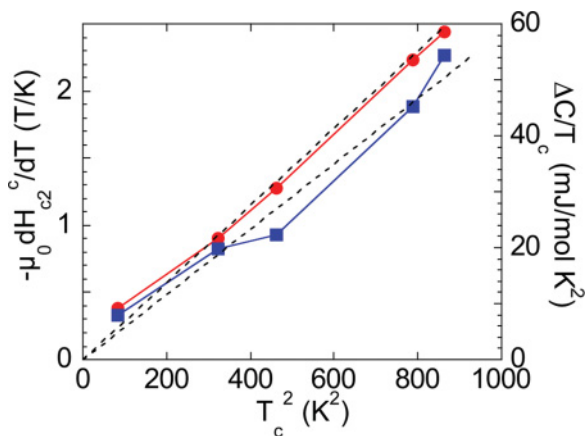


FIG. 4. (Color online) Dependence of the upper critical field slope and of the specific heat anomaly on T_c^2 .

and additional uncertainties may arise due to varying sample quality and approximations made to extract the jump height²² as well as due to the definition of T_c (entropy conserving construction, peak position of $\Delta C/T$, or onset of $\Delta C/T$), a trend extending over a large number of 122-, 111-, and 11-based samples is clearly seen. It is remarkable that the $\Delta C/T_c$ vs T_c^2 correlation is observed for electron, hole, and isovalent doped [such as $\text{BaFe}_2(\text{As}_{1-x}\text{P}_x)_2$ presented here] materials. In addition, the BNC scaling occurs for underdoped and overdoped compounds as well as in clean samples, i.e., $\text{BaFe}_2(\text{As}_{1-x}\text{P}_x)_2$, and in strongly scattering charge doped compounds. A notable exception from this scaling is Sm-1111 (Ref. 17) for which the specific heat anomaly is roughly a factor of 10 too small as compared to the BNC scaling.

Assuming that the $\Delta C/T_c$ vs T_c^2 line indeed represents a general property of a large class of Fe-based superconductors, then our results on $\text{BaFe}_2(\text{As}_{1-x}\text{P}_x)_2$ put constraints

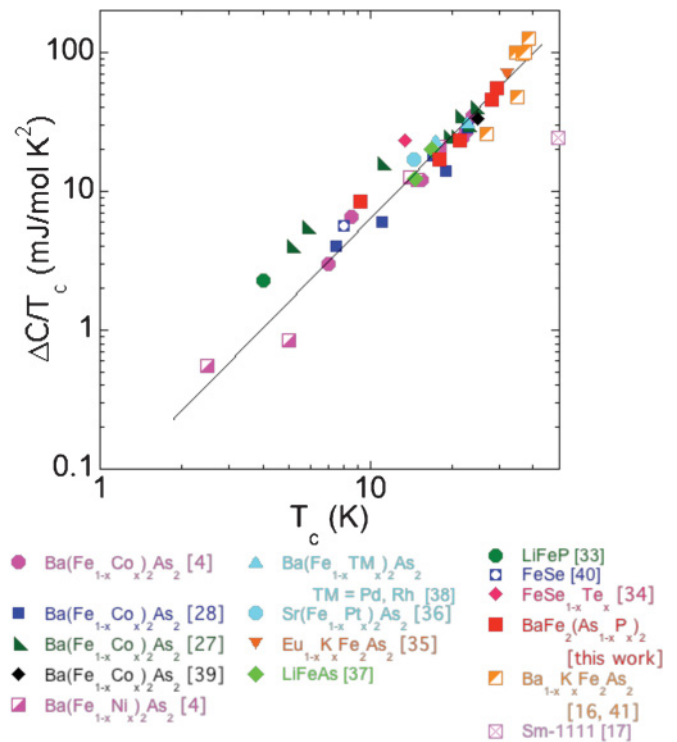


FIG. 5. (Color) Compilation of $\Delta C/T_c$ vs T_c values of various Fe-based superconductors plotted on log-log scales (reference numbers are in brackets). The line indicates a quadratic dependence. See also Refs. 5, 6, and 22.

on models that have been advanced to account for the scaling. For instance, recognizing that within the conventional weak-coupling BCS framework the $\Delta C/T_c$ vs T_c^2 scaling implies a very peculiar balance of materials parameters, Zaanen²³ suggested non-Fermi liquid behavior in order to account for the wide occurrence of this scaling. However, dHvA experiments^{7,8} on overdoped $\text{BaFe}_2(\text{As}_{1-x}\text{P}_x)_2$ yielded a Fermi surface topology in reasonable agreement with band-structure calculations implying that at least this material can be described as Fermi liquid. Furthermore, Kogan²¹ has pointed out that the T_c^2 variation can arise when strong pair-breaking scattering induces a gapless superconducting state. Pair-breaking scattering could arise naturally in superconductors with sign-changing order parameter such as s^\pm gap symmetry due to nonmagnetic interband scattering.²⁴ In the case of $\text{BaFe}_2(\text{As}_{1-x}\text{P}_x)_2$, however, the overdoped samples have reduced T_c and $\Delta C/T_c$, but at the same time enhanced electron mean free paths, that is, reduced scattering,^{7-9,29} which is at odds with the theoretical model. Vavilov *et al.*²⁶ developed a model for the specific heat of underdoped compounds based on the coexistence of spin-density wave (SDW) and superconducting order. This model, however, does not account for the data in the overdoped regime. Recent specific heat measurements^{27,28} on $\text{Ba}(\text{Fe}_{1-x}\text{Co}_x)_2\text{As}_2$ revealed sizable residual terms γ_r in the low-temperature specific heat, that is, a contribution to the electronic specific heat arising from unpaired electrons, which shows a clear anticorrelation with T_c and ΔC : γ_r is minimal at optimum doping and increases significantly on under- and overdoping. The entropy loss due to γ_r could account for the rapid decrease of $\Delta C/T_c$ away from optimum doping. The origins of the γ_r term have not been clarified yet. Since nonmagnetic interband scattering in a s^\pm superconductor is pair breaking,²⁴ scattering off charged dopant sites could induce quasiparticle states in the gap contributing to a residual γ_r term. However, it is not obvious why this process would lead to a dependence of γ_r and $\Delta C/T_c$ that is nonmonotonous in Co concentration. Alternatively, a “Swiss cheese” model has been invoked²⁷ in which a region of the size of the coherence length around a defect site is driven normal thereby contributing to the residual electronic specific heat. This model has been applied to high- T_c (Ref. 29) and heavy Fermion³⁰ materials. Since the coherence length is typically the smallest for the highest T_c , that is, at optimum doping, a nonmonotonous variation of γ_r with dopant concentration could arise.

For the optimally doped compound we obtain a Ginzburg-Landau penetration depth (linear extrapolation of $1/\lambda^2$ to zero temperature) of $\lambda_{GL}^{ab}(0) \approx 101$ nm. Assuming the empirical two-fluid temperature dependence would yield a

zero-temperature penetration depth of $\lambda_{ab}(0) = 2\lambda_{GL}^{ab}(0) \approx 200$ nm, which is in good agreement with measurements based on microwave surface resistance.¹² With increasing P doping, that is, decreasing T_c , the penetration depth increases, implying a decrease of the lower critical field H_{c1} . This appears as a natural result; however, it has been noted³¹ that with doping the effective mass m^* on the electron Fermi surface sheets decreases⁷ and at the same time the carrier concentration n (of one polarity) increases and that therefore the superfluid density $n/m^* \approx 1/\lambda^2$ would increase, corresponding to a decrease of λ . This apparent contradiction may arise from the fact that our measurements yield values of the slopes of H_{c2} and $1/\lambda^2$ near T_c where GL theory applies and that due to multiband effects the actual temperature dependence of λ deviates from the two-fluid form as evidenced by a pronounced inflection point in $1/\lambda^2(T)$.^{12,32} A quantitative evaluation of the doping dependence of the low-temperature penetration depth will require the determination of the Fermi surface averages of the gap function and of the Fermi velocity on all sheets of realistic Fermi surfaces. We note though that due to the strong decrease of κ_c with decreasing T_c , the relative increase of λ_{GL}^{ab} is significantly smaller than that of the coherence length.

In conclusion, we present a systematic study of the specific heat transitions on a series of $\text{BaFe}_2(\text{As}_{1-x}\text{P}_x)_2$ single crystals with phosphorus doping ranging from near-optimum doped $x = 0.3$ to strongly overdoped $x = 0.55$. $\text{BaFe}_2(\text{As}_{1-x}\text{P}_x)_2$ is the first member of the Fe-based layered superconductors that follows the BNC scaling of the specific heat transition remarkably and—at the same time—can be made with very high purity. The high purity of this material imposes additional restraints on theories aimed at explaining the scaling since models based on specific electron scattering mechanisms appear to be inconsistent with our results. Furthermore, we find that the Ginzburg-Landau parameter κ_c decreases significantly with doping whereas the superconducting anisotropy is $\Gamma \approx 2.6$, independent of doping, indicative of the dominating role of the electron Fermi surface sheets in forming the superconducting state.

Crystal synthesis was supported by the Center for Emergent Superconductivity, an Energy Frontier Research Center funded by the US Department of Energy, Office of Science, Office of Basic Energy Sciences (C.C., L.F., W.K.K.). Materials characterization was supported by the core research program of the US Department of Energy, Office of Science, Office of Basic Energy Sciences (U.W., H.C., G.W.C.), under Contract No. DE-AC02-06CH11357. We acknowledge helpful discussions with V. Kogan, T. Shibauchi, and M. Graf.

¹K. Kadowaki and S. B. Woods, *Solid State Commun.* **58**, 507 (1986); A. C. Jacko, J. O. Fjærestad, and B. J. Powell, *Nat. Phys.* **5**, 422 (2009).

²Y. J. Uemura *et al.*, *Phys. Rev. Lett.* **62**, 2317 (1989).

³C. C. Homes, S. V. Dordevic, M. Strongin, D. A. Bonn, R. Liang, W. N. Hardy, S. Komiya, Y. Ando, G. Yu, N. Kaneko, X. Zhao, M. Greven, D. N. Basov, and T. Timusk, *Nature* **430**, 539 (2004); J. J.

Tu, J. Li, W. Liu, A. Punnoose, Y. Gong, Y. H. Ren, L. J. Li, G. H. Cao, Z. A. Xu, and C. C. Homes, *Phys. Rev. B* **82**, 174509 (2010).

⁴S. L. Bud'ko, N. Ni, and P. C. Canfield, *Phys. Rev. B* **79**, 220516 (2009).

⁵J. Paglione and R. L. Greene, *Nat. Phys.* **6**, 645 (2010); P. C. Canfield and S. L. Bud'ko, *Annu. Rev. Condens. Matter Phys.* **1**, 27 (2010).

- ⁶J. S. Kim, P. J. Hirschfeld, G. R. Stewart, S. Kasahara, T. Shibauchi, T. Terashima, and Y. Matsuda, *J. Phys.: Condens. Matter* **23**, 222201 (2011); *Phys. Rev. B* **81**, 214507 (2010).
- ⁷H. Shishido, A. F. Bangura, A. I. Coldea, S. Tonegawa, K. Hashimoto, S. Kasahara, P. M. C. Rourke, H. Ikeda, T. Terashima, R. Settai, Y. Ōnuki, D. Vignolles, C. Proust, B. Vignolle, A. McCollam, Y. Matsuda, T. Shibauchi, and A. Carrington, *Phys. Rev. Lett.* **104**, 057008 (2010).
- ⁸J. G. Analytis, J. H. Chu, R. D. McDonald, S. C. Riggs, and I. R. Fisher, *Phys. Rev. Lett.* **105**, 207004 (2010).
- ⁹L. Fang, Y. Jia, J. A. Schlueter, A. Kayani, Z. L. Xiao, H. Claus, U. Welp, A. E. Koshelev, G. W. Crabtree, and W. K. Kwok, *Phys. Rev. B* **84**, 140504 (2011).
- ¹⁰M. Yamashita, Y. Senshu, T. Shibauchi, S. Kasahara, K. Hashimoto, D. Watanabe, H. Ikeda, T. Terashima, I. Vekhter, A. B. Vorontsov, and Y. Matsuda, *Phys. Rev. B* **84**, 060507 (2011).
- ¹¹Y. Nakai, T. Iye, S. Kitagawa, K. Ishida, H. Ikeda, S. Kasahara, H. Shishido, T. Shibauchi, Y. Matsuda, and T. Terashima, *Phys. Rev. Lett.* **105**, 107003 (2010).
- ¹²K. Hashimoto, M. Yamashita, S. Kasahara, Y. Senshu, N. Nakata, S. Tonegawa, K. Ikada, A. Serafin, A. Carrington, T. Terashima, H. Ikeda, T. Shibauchi, and Y. Matsuda, *Phys. Rev. B* **81**, 220501 (2010).
- ¹³Y. Zhang, Z. R. Ye, Q. Q. Ge, F. Chen, Juan Jiang, M. Xu, B. P. Xie, and D. L. Feng, *Nat. Phys.* **8**, 371 (2012).
- ¹⁴K. Vandervoort, G. Griffith, H. Claus, and G. W. Crabtree, *Rev. Sci. Instrum.* **62**, 2271 (1991).
- ¹⁵S. Tagliati, A. Rydh, R. Xie, U. Welp, and W. K. Kwok, *J. Phys.: Conf. Ser.* **150**, 052256 (2009); S. Tagliati and A. Rydh, *Thermochim. Acta* **522**, 66 (2011).
- ¹⁶U. Welp, R. Xie, A. E. Koshelev, W. K. Kwok, H. Q. Luo, Z. S. Wang, G. Mu, and H. H. Wen, *Phys. Rev. B* **79**, 094505 (2009).
- ¹⁷U. Welp, C. Chaparro, A. E. Koshelev, W. K. Kwok, A. Rydh, N. D. Zhigadlo, J. Karpinski, and S. Weyeneth, *Phys. Rev. B* **83**, 100513 (2011).
- ¹⁸Z. Pribulova, T. Klein, J. Kacmarcik, C. Marcenat, M. Konczykowski, S. L. Budko, M. Tillman, and P. C. Canfield, *Phys. Rev. B* **79**, 020508 (2009); U. Welp, R. Xie, A. E. Koshelev, W. K. Kwok, P. Cheng, L. Fang, and H. H. Wen, *ibid.* **78**, 140510 (2008).
- ¹⁹K. Suzuki, H. Usui, and K. Kuroki, *J. Phys. Soc. Jpn.* **80**, 013710 (2011).
- ²⁰B. J. Arnold, S. Kasahara, A. I. Coldea, T. Terashima, Y. Matsuda, T. Shibauchi, and A. Carrington, *Phys. Rev. B* **83**, 220504 (2011).
- ²¹V. G. Kogan, *Phys. Rev. B* **80**, 214532 (2009); **81**, 184528 (2010).
- ²²G. R. Stewart, *Rev. Mod. Phys.* **83**, 1589 (2011).
- ²³J. Zaanen, *Phys. Rev. B* **80**, 212502 (2009).
- ²⁴S. Onari and H. Kontani, *Phys. Rev. Lett.* **103**, 177001 (2009); A. Glatz and A. E. Koshelev, *Phys. Rev. B* **82**, 012507 (2010).
- ²⁵S. Kasahara, T. Shibauchi, K. Hashimoto, K. Ikada, S. Tonegawa, R. Okazaki, H. Shishido, H. Ikeda, H. Takeya, K. Hirata, T. Terashima, and Y. Matsuda, *Phys. Rev. B* **81**, 184519 (2010).
- ²⁶M. G. Vavilov, A. V. Chubukov, and A. B. Vorontsov, *Phys. Rev. B* **84**, 140502(R) (2011).
- ²⁷F. Hardy, P. Burger, T. Wolf, R. A. Fisher, P. Schweiss, P. Adelman, R. Heid, R. Fromknecht, R. Eder, D. Ernst, H. v. Löhneysen, and C. Meingast, *Europhys. Lett.* **91**, 47008 (2010).
- ²⁸G. Mu, Zeng Bin, Cheng Peng, Wang Zhao-Sheng, Fang Lei, Shen Bing, Shan Lei, Ren Cong, and Wen Hai-Hu, *Chin. Phys. Lett.* **27**, 037402 (2010).
- ²⁹B. Nachumi, A. Keren, K. Kojima, M. Larkin, G. M. Luke, J. Merrin, O. Tchernyshöv, Y. J. Uemura, N. Ichikawa, M. Goto, and S. Uchida, *Phys. Rev. Lett.* **77**, 5421 (1996).
- ³⁰E. D. Bauer, Y.-f. Yang, C. Capan, R. R. Urbano, C. F. Miclea, H. Sakai, F. Ronning, M. J. Graf, A. V. Balatsky, R. Movshovich, A. D. Bianchi, A. P. Reyes, P. L. Kuhns, J. D. Thompson, and Z. Fisk, *Proc. Natl. Acad. Sci. USA* **108**, 6857 (2011).
- ³¹T. Shibauchi (private communication).
- ³²V. G. Kogan, *Phys. Rev. B* **80**, 214532 (2009); A. B. Vorontsov, M. G. Vavilov, and A. V. Chubukov, *ibid.* **79**, 140507 (2009); R. Prozorov and V. G. Kogan, *Rep. Prog. Phys.* **74**, 124505 (2011).
- ³³Z. Deng, X. C. Wang, Q. Q. Liu, S. J. Zhang, Y. X. Lv, J. L. Zhu, R. C. Yu, and C. Q. Jin, *Europhys. Lett.* **87**, 37004 (2009).
- ³⁴D. Braithwaite, G. Lapertot, W. Knaf, and I. Sheikin, *J. Phys. Soc. Jpn.* **79**, 053703 (2010).
- ³⁵H. S. Jeevan and P. Gegenwart, *J. Phys.: Conf. Ser.* **200**, 012060 (2010).
- ³⁶K. Kirshenbaum, S. R. Saha, T. Drye, and J. Paglione, *Phys. Rev. B* **82**, 144518 (2010).
- ³⁷U. Stockert, M. Abdel-Hafiez, D. V. Evtushinsky, and V. B. Zabol, *Phys. Rev. B* **83**, 224512 (2011); B. S. Lee, S. H. Khim, J. S. Kim, G. R. Stewart, and K. H. Kim, *Europhys. Lett.* **91**, 67002 (2010).
- ³⁸N. Ni, A. Thaler, A. Kracher, J. Q. Yan, S. L. Budko, and P. C. Canfield, *Phys. Rev. B* **80**, 024511 (2009); K. Gofryk, A. S. Sefat, M. A. McGuire, B. C. Sales, D. Mandrus, T. Imai, J. D. Thompson, E. D. Bauer, and F. Ronning, *J. Phys.: Conf. Ser.* **273**, 12094 (2011).
- ³⁹J.-H. Chu, J. G. Analytis, C. Kucharczyk, and I. R. Fisher, *Phys. Rev. B* **79**, 014506 (2009).
- ⁴⁰F.-C. Hsu, J.-Y. Luo, K.-W. Yeh, T.-K. Chen, T.-W. Huang, P. M. Wu, Y.-C. Lee, Y.-L. Huang, Y.-Y. Chu, D.-C. Yan, and M.-K. Wu, *Proc. Natl. Acad. Sci. USA* **105**, 14262 (2008).
- ⁴¹N. Ni, S. L. Budko, A. Kreyssig, S. Nandi, G. E. Rustan, A. I. Goldman, S. Gupta, J. D. Corbett, A. Kracher, and P. C. Canfield, *Phys. Rev. B* **78**, 014507 (2008); G. Mu, H. Luo, Z. Wang, L. Shan, C. Ren, and H. H. Wen, *ibid.* **79**, 174501 (2009); M. Rotter, M. Tegel, I. Schellenberg, F. M. Schappacher, R. Pöttgen, J. Deisenhofer, A. Günther, F. Schrettle, A. Loidl, and D. Johrendt, *New J. Phys.* **11**, 025014 (2009); P. Popovich, A. V. Boris, O. V. Dolgov, A. A. Golubov, D. L. Sun, C. T. Lin, R. K. Kremer, and B. Keimer, *Phys. Rev. Lett.* **105**, 027003 (2010).